Optical and Quantum Electronics (2024) 56:1249
https://doi.org/10.1007/s11082-024-07128-6

Band structure study of pure and doped anatase titanium dioxide (TiO_2) using first-principle-calculations: role of atomic mass of transition metal elements (TME) on band gap reduction

Taha Yasin Ahmed[1] · Omed Gh. Abdullah[2] · Soran M. Mamand[2] · Shujahadeen B. Aziz[3,4]

Received: 2 February 2024 / Accepted: 21 May 2024 / Published online: 26 June 2024

Abstract
The titanium dioxide (TiO_2) semiconductor's wide band gap property restricts its application in a variety of fields. To ensure cost-effectiveness and time efficiency, researchers emphasized material modeling and theoretical analysis. This study employs a Density Functional Theory approach to investigate how the presence of transition metal elements (TME) like rhodium (Rh) and rhenium (Re) affects the optoelectronic properties of TiO_2. The study was carried out using the VASP software package and the plane-wave pseudopotential technique. The formation energy, electronic band structure, and optical properties of TiO_2 were affected by the addition of both Rh and Re as doping materials. The outcomes of the band structure and total density of states (TDOS), point out notable alterations in the energy gap (E_g) of TiO_2. The plot of the band structure illustrates that the introduction of Re leads to a more substantial reduction in the TiO_2 band gap compared to Rh. The introduction of numerous sub-states into the band gap causes the valence band to approach the conduction band at the Gamma point. The band gap reduction caused by the addition of Rh and Re TME is confirmed by the relocation of the TDOS to lower energies in the doped TiO_2 structure. Furthermore, significant changes in the partial density of states of TiO_2 upon Re doping have been observed at the bottom of the conduction band, highlighting the effectiveness of Re doping in modifying the electronic band structure of TiO_2. The outcomes of band structure and TDOS proved that TME with high atomic mass is certain to decrease TiO_2's band gap to the range required for usage as a photocatalytic material. Rh and Re doping in TiO_2 alter their optical properties, making them suitable for optoelectronic devices.

Keywords VASP · DFT · Band structure · DOS · Linear optical properties

Extended author information available on the last page of the article

1 Introduction

The photoelectrochemical splitting of water on titanium dioxide (TiO_2) electrodes has sparked significant interest in TiO_2 as a highly promising photocatalytic material. This is mainly due to its cost-effectiveness, non-toxic nature, and long-term stability against corrosion (Hoffmann et al. 1995). unfortunately, TiO_2 suffers from a notable efficiency drawback as it can only respond to ultraviolet light, which constitutes less than 5% of the total solar energy spectrum (Chen et al. 2018). This limitation arises from its intrinsic band gap, which is reported to be 3.2 eV for anatase (Yu et al. 2015; Samsudin and Hamid 2017; Sharma et al. 2023). Consequently, numerous approaches have been suggested to overcome this limitation and enhance the photocatalytic efficiency of TiO_2 within the visible spectra region of electromagnetic waves. Hopefully, a doping technique has been broadly studied and established to be an effective solution for extending the range of spectral response of TiO_2 and improving its photocatalytic performance (Ma and Sauer 2013; Mazierski et al. 2019; Ruiz et al. 2023; Nair et al. 2022; Patil et al. 2019).

Farzaneh et al. (2022) employed density functional theory (DFT) in their investigation of aluminum (Al) and copper (Cu) substitutional doping in anatase TiO_2, aiming to optimize the utilization of a broad spectral range during solar irradiation by producing anatase TiO_2 with lower band gaps. In a study by Tian and Liu (2006), they conducted calculations involving substitutional S doping at the Ti site, resulting in a reduction of the band gap in anatase TiO_2, with a red shift of the absorption edge. In their work, Ye et al. (2023) utilized first-principles density functional theory to compute and model the electronic band structure and associated optical characteristics of intrinsic and various rare earth elements (La, Ce, Hf, and Pr) doped anatase TiO_2. The computed outcomes reveal that the energy band gap values of the doped samples are narrower compared to pure TiO_2. Among these, Ce-doped anatase TiO_2 exhibits the smallest band gap, measuring 1.756 eV, and displays a notable enhancement in its light absorption efficiency within the visible spectrum. Numerous studies have shown that by using appropriate dopants, the band of TiO_2 can be engineered, making it a better visible light-active photocatalyst (Muthukrishnan et al. 2023).

TiO_2 exists in three different crystalline forms: one rhombic form called brookite and two tetragonal forms known as rutile and anatase (Eddy et al. 2023; Verma et al. 2017). Obtaining brookite in laboratory conditions is difficult, whereas rutile and anatase are more readily prepared. In its bulk form, rutile represents the stable phase. However, the anatase structure is typically favored when using solution-phase preparation methods for TiO_2. The two main factors that explain these observations are the material's surface energy and the chemistry of its formation (Mazierski et al. 2019). It has been discovered that the surface energy of anatase is lower than that of brookite and rutile (Coronado et al. 2008). The diverse range of experimental conditions employed to synthesize various TiO_2 phases is a complicating factor in comprehending nanoparticle formation. This variation makes it challenging to accurately compare and analyze the underlying mechanisms (Kondamareddy et al. 2018).

Optoelectronics has witnessed remarkable advancements in recent years due to its potential applications in various cutting-edge technologies, such as photovoltaics, light-emitting devices, and sensors (Zhang et al. 2022; Liu et al. 2022). One of the key strategies for optimizing the performance of optoelectronic structures lies in the incorporation of functional nanomaterials. TiO_2, being a prominent semiconductor material, has garnered significant attention due to its exceptional electronic and optical properties (Ahmed and Hasan 2023; Armakovic et al. 2023). Integrating TiO_2 with metal elements presents an

intriguing prospect for tailoring the optoelectronic behavior of metal-based devices, potentially leading to superior performance and enhanced efficiency.

This research delves into the influence of introducing Re and Rh elements on the optoelectronic properties of TiO2 using comprehensive first-principles simulations. Precisely, the study utilizes the Vienna Ab initio Simulation Package (VASP) and employs the plane-wave pseudopotential method in conjunction with density functional theory (DFT). DFT is a common ab initio technique. Concerning several material properties, such as equilibrium material structure, electronic band structure, and phonon properties, it may successfully predict them given the initial unit cell structure. The frequency-dependent dielectric function may be computed using these results in the dielectric function models. Then, using EM theory, bulk materials' and nanostructures' radiative characteristics can be calculated (Bao and Ruan 2010). This powerful combination of computational tools offers a highly accurate and reliable approach for analyzing electronic structure, optical properties, and charge transport mechanisms of materials at the atomic level. Thus, the study focused on investigating the charge transport properties of the doped TiO_2 system, including conductivity and optical dielectric constant. A thorough understanding of the charge transport behavior is imperative in designing efficient optoelectronic devices and elucidating the charge transfer mechanisms between TiO_2 and dopant elements.

2 Computational method and theoretical description

The VASP which is based on DFT and uses a plane-wave pseudopotential approach, was used in this calculation (Hafner 2008, 2007). The exchange–correlation (XC) interaction was characterized using the generalized gradient approximation (GGA) within the Perdew-Burke-Ernzerhof for solids (PBEsol) approach (Perdew et al. 1996, 2008). All calculations, including those involving Band Structure (BS), Density Of States (DOSs), and Optical Properties (OPs), employ this function. The energy of XC (E_{XC}) is a function of density and its gradient in GGA. The GGA overestimates lattice constants while underestimating energy band gaps. This is because GGA interprets electron–electron correlations wrongly, which are particularly pronounced in strongly correlated materials like TiO_2 (Perdew et al. 1996). The DFT + U approach, also known as mean-field Hubbard correction, attempts to solve this self-interaction problem by introducing a repellent on-site potential U (Anisimov et al. 1991). Consequently, we utilize the GGA + U approach in which the d-orbitals of Ti, Rh, and Re, respectively, have Hubbard potential U values of 8.5, 7, and 7 eV (Rasul et al. 2022; Tesch and Kowalski 2022).

Figure 1a shows the structure of anatase TiO_2 in which titanium (Ti) atoms and six oxygen (O) atoms are bonded, each oxygen atom bonds to three titanium atoms, forming an octahedral geometry. Tetragonal ($P4_2/mnm$ space group) primitive unit cell of anatase TiO_2 has lattice parameters with values of a = b = 3.79925 Å and c = 9.56435 Å, consistent with the experimental data (Howard et al. 1991; Maeda and Yamada 2007). This TiO2 anatase structure's conventional unit cell is used to create a super-cell with dimensions $2 \times 2 \times 1$, as shown in Fig. 1b. It has 48 atoms in total (Ti_nO_{2n}) and is restricted to the condition n + 2n = N.

In this study, the substitutional technique is taken into account. Since the Ti and Rh (Re) atoms have comparable radii, replacing a Ti atom with a Rh (Re) atom is better energetically than replacing an O atom. To reduce interference between periodic images of the dopant atoms, our supercells only have one dopant atom (Taylor and Bruneval 2011). This

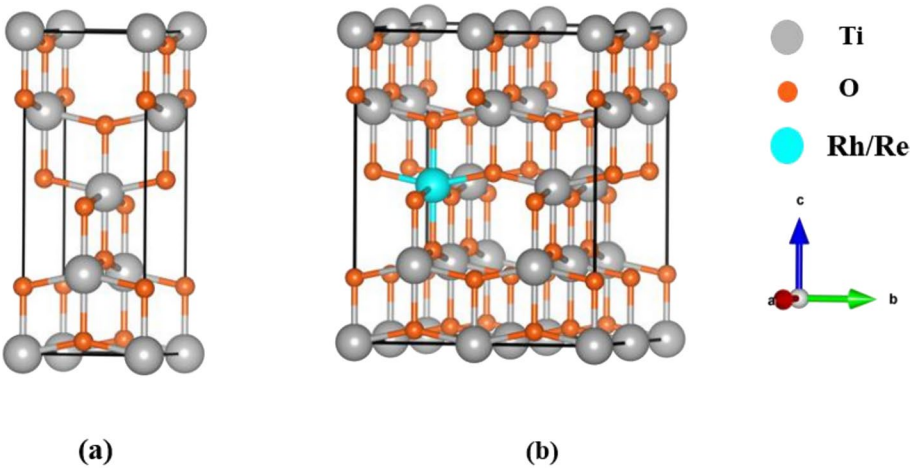

Fig. 1 **a** The typical unit cells of anatase TiO_2 structures depicted using a ball-and-stick representation. The Ti and O atoms are colored gray and orange, respectively, **b** the 2×2x1 super-cell contains 48 atoms with $Ti_{15}Rh(Re)O_{32}$ configuration. Dopant concentration: 6.25%

creates the structure $Ti_{n-1}X_1O_{2n}$, where X is the doping element. This means a doped system with $Ti_{15}Rh(Re)O_{32}$ configuration for our super-cell. This translates to a corresponding doping concentration of 6.25%, as demonstrated in Fig. 1b. The energy convergence test indicates a system's stability. The doped TiO_2 systems' lattice constants and substitutional atom positions are optimized. According to the convergence test, the plane-wave cutoff kinetic energy remains consistent at 570 eV for both the pure and doped systems. Monkhorst–Pack was used for the Brillouin zone k-point sampling 12×12x10 and 15×15x10 for pure and doped systems, respectively (Monkhorst and Pack 1976). In the optimization process, energy, energy change, force convergence, and maximum displacement tolerances are 3.5×10^2 eV, 6.3×10^{-2} eV, 3.5×10^2 eV/ Å and 1×10^{-4} Å, respectively.

3 Results and discussion

3.1 Band structures and density of states

The analysis of the physical characteristics of materials heavily relies on the electronic properties, including the electronic band structure (EBS) and DOS. These electronic characteristics provide valuable insights into how materials interact with light and other external stimuli, impacting their overall behavior and functionalities. The EBS provides crucial insights into the energy ranges, known as energy bands, where electrons have a probability of occupying. It also identifies energy ranges that cannot be occupied, referred to as the band gap. This band gap is significant as it influences the electrical and optical properties (Ops) of materials, including their conductivity and ability to absorb or emit light (Sarkar et al. 2023; Ullah et al. 2024). Understanding the electronic band structure is crucial in predicting and interpreting the behavior of electrons in materials, making it an essential aspect of material analysis in various scientific and technological fields (Raia et al. 2023). For semiconductors and insulators, determining the electronic band gap involves computing

the difference between the energy levels of the conduction band minimum (CBM) and the valence band maximum (VBM). Calculations of electronic band structure offer an understanding of the possible electronic transitions from the VBM to the CBM (Williamson et al. 2017). Figures 2 and 3 display the electronic band structure outcomes for pure TiO_2 and TiO_2 doped with Rh (or Re), respectively, along the same direction in the Brillouin zone.

In both figures, to calculate the value of energy band gap CBm and the VBM are designated. The band gap value of the pure TiO_2 is 3.20 eV, while the band gap values of both Rh and Re-doped TiO_2 are 1.90 and 0.20 eV, respectively. This is effective in making an efficient optoelectronic material based on TiO_2. The pure TiO_2 band gap value (Fig. 2a) is comparable with that of the experimental value (Yu et al. 2013; Ahmed et al. 2021). It's interesting to note that in the EBS of doped TiO_2, the CBm and the top of the valence band (VB) both reside at the same position, indicating the direct band gap transition in the doped samples, making it more favorable for certain optoelectronic applications like light emission or absorption. The direct band gap property is significant as it affects the material's ability to efficiently interact with photons and participate in various optical processes. The reduction of the band gap in TiO_2 upon doping clarifies that when exposed to light illumination, Rh(Re) doped TiO_2 displays improved photocatalytic activity and photoconductivity. This decrease in band gap allows the material to efficiently absorb a broader range of photons, enabling more effective utilization of light energy for photocatalytic processes and promoting better photo-conductive behavior. These improved properties make Rh(Re) doped TiO_2 a promising candidate for various prospective applications in photocatalysis and optoelectronics (Chen et al. 2012; Ma et al. 2020).

It's remarkable to note that the changes in atomic mass influence significantly the band gap. The result of the current work indicates that the band gap decreases more

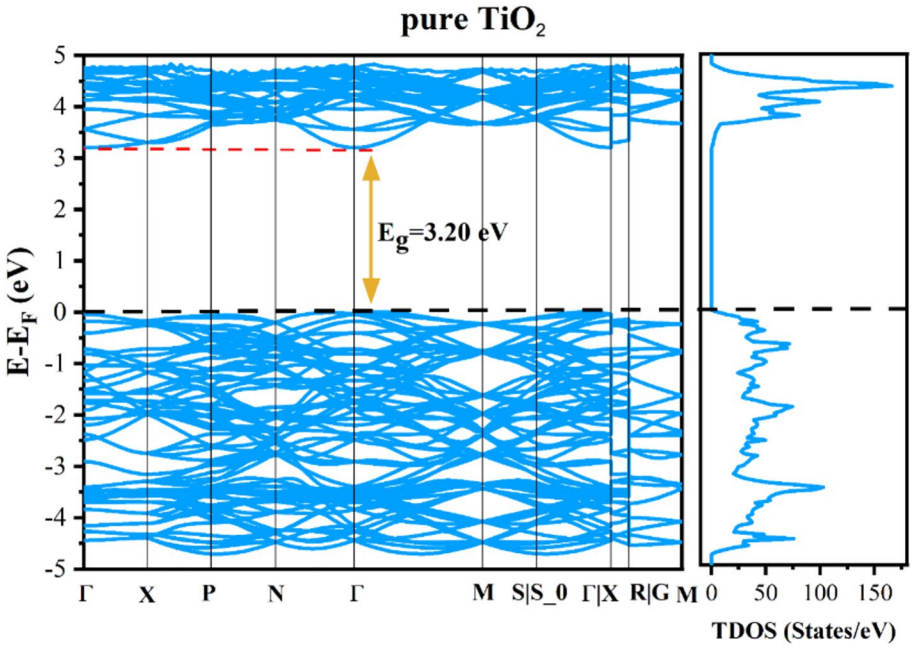

Fig. 2 Band structure and TDOS of pure TiO_2 anatase

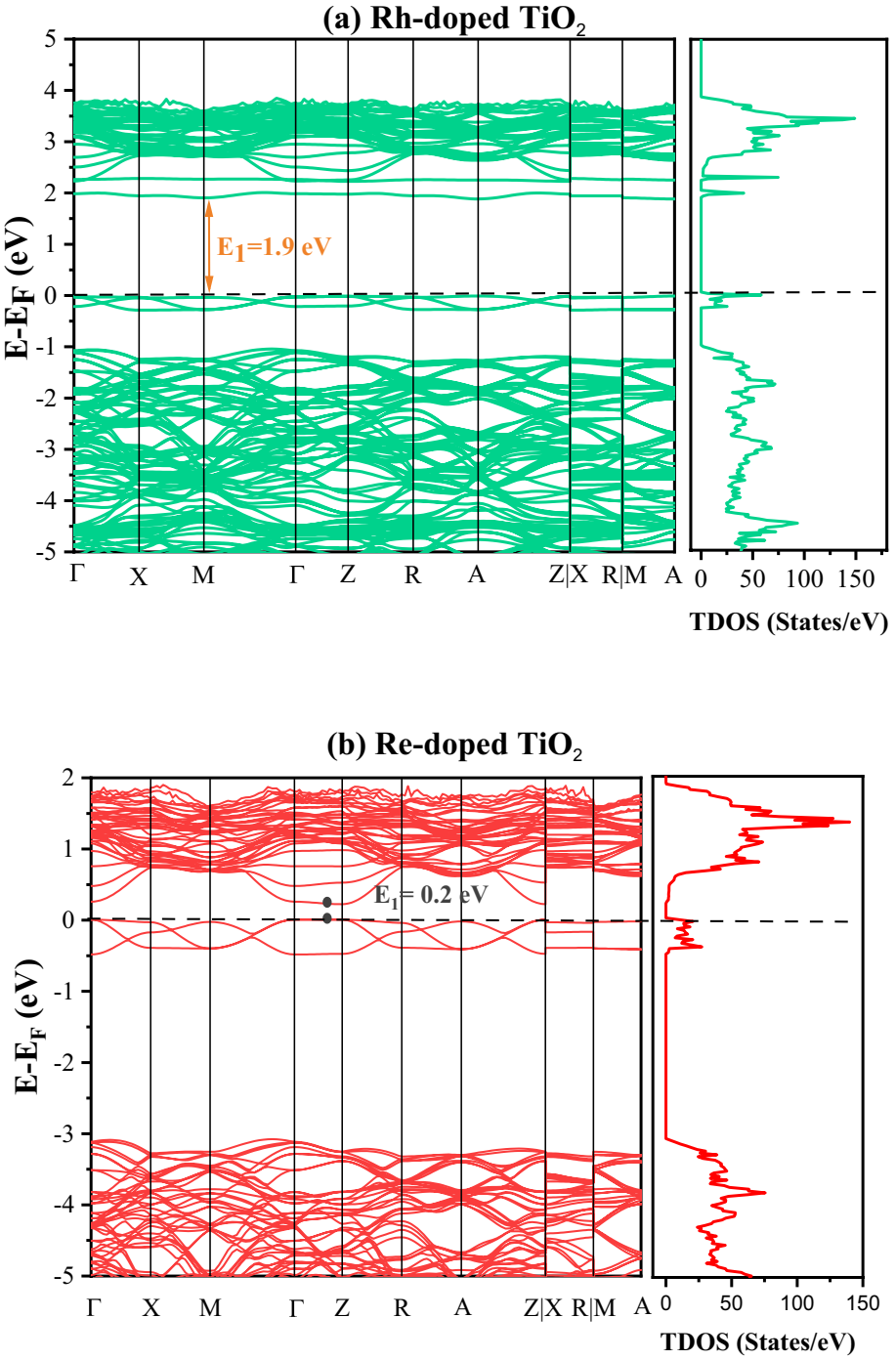

Fig. 3 Band structure and TDOS of **a** Rh-doped TiO_2 and **b** Re-doped TiO_2 structures

significantly with higher atomic mass. The results of pure TiO_2 compared to TiO_2 doped with Re and Rh established the fact that the band gap reduction is more favorable with Re doping due to its higher atomic mass (186.207 amu) compared to Rh (102.9055 amu). To our knowledge the atoms of higher atomic radius such as Re will relocate efficiently within the structure of TiO_2 and due to their higher atomic mass will provide more electrons compared to lower atomic mass elements of the periodic table. Consequently, the band structure analysis achieved in the present study demonstrates that transition metal elements (TME) with higher atomic masses successfully diminish TiO_2's band gap, rendering it appropriate for application as a photocatalytic material. Furthermore, the electronic configuration of elements of the periodic table may support our assumptions. For example, Re, with an atomic number of 75 and an electron configuration of [Xe] $4f^{14}5d^{5}6s^{2}$, possesses 2 valence electrons, whereas Rh, with an atomic number of 45 and an electron configuration of [Kr] $4d^{8}5s^{1}$, has 1 valence electron. Consequently, the inequality in valence electrons (VEs) may influence the band gap. The TME with higher valence electrons contributes significantly to the introduction of more impurity states within the band gap, thereby reducing the TiO_2's band gap efficiently. The higher number of VEs in Re compared to Rh results in Re being more effective in reducing TiO_2's band gap (Schwarz 2010; Shabalin and Rhenium. 2014).

Most of the published data showed a similar trend for the reduction in energy band gap for doped anatase TiO_2 (Tian and Liu 2006; Ye et al. 2023; Liu et al. 2014). Ghuman and Singh (2013) also reported that red shifting in Rh-doped rutile TiO_2 results from charge transfer occurring between Rh and TiO_2 conduction or valence bands; or due to d-d transitions within the crystal field. Nonetheless, these mid-gap states come with a drawback since they can function as recombination centers, consequently leading to a notable decline in photocatalytic efficiency (Rasul et al. 2022). According to Niishiro et al. (2007), this recombination is predominantly attributed to the creation of Rh^{4+}.

To show the establishment of the EBS of pure and Rh(Re) doped TiO_2, the Partial Density Of States (PDOS) diagrams are shown in Fig. 4. A comprehensive understanding of the composition and origin of the calculated bands can be attained by thoroughly analyzing the PDOS. The reference point for the Fermi level is established at zero. In Fig. 4a, the PDOS of pure TiO_2 is depicted. It is evident that the valence band (VB) is composed of upper and lower bands. The lower VB is primarily influenced by O-2 s orbitals spanning from −15.9 to −17.5 eV, while the upper VBs close to the Fermi energy are mainly contributed by O-2p and Ti-3d orbitals, ranging from −4.7 to 0 eV. Additionally, the conduction bands (CBs) are influenced by Ti-3d and O-2p orbitals, situated within the energy range of 3.2 to 4.8 eV. As a result, one can say that, the O-2p mainly dominates the VB, and the CB is primarily correlated with the Ti-3d (Zhu et al. 2014). The findings confirm a significant hybridization occurring between the O-2p and Ti-3d states in proximity to the CB. Furthermore, the energy range from 0 to 3.2 eV constitutes the band gap. The PDOS of Rh and Re-doped TiO_2 are shown in Fig. 4b, c. It's noticeable that a distinct region is formed between the Fermi energy and the upper valence band. Furthermore, the conduction bands are notably lowered, extending to lower energy levels. However, the introduction of Rh atoms' 4d orbitals leads to a reduction in the energy gap, as illustrated in Fig. 4b. It is evident that in the case of Re-doped TiO_2, the distinct region becomes more pronounced and the conduction bands are further lowered, extending to even lower energy levels which caused to decrease in band bap compared to Rh-doped TiO_2. This effect is depicted in Fig. 4c. Furthermore, the states of Ti from the VB lie near 3 eV, while the states Rh and Re contribute in the VB ranges from 5 to 8 eV.

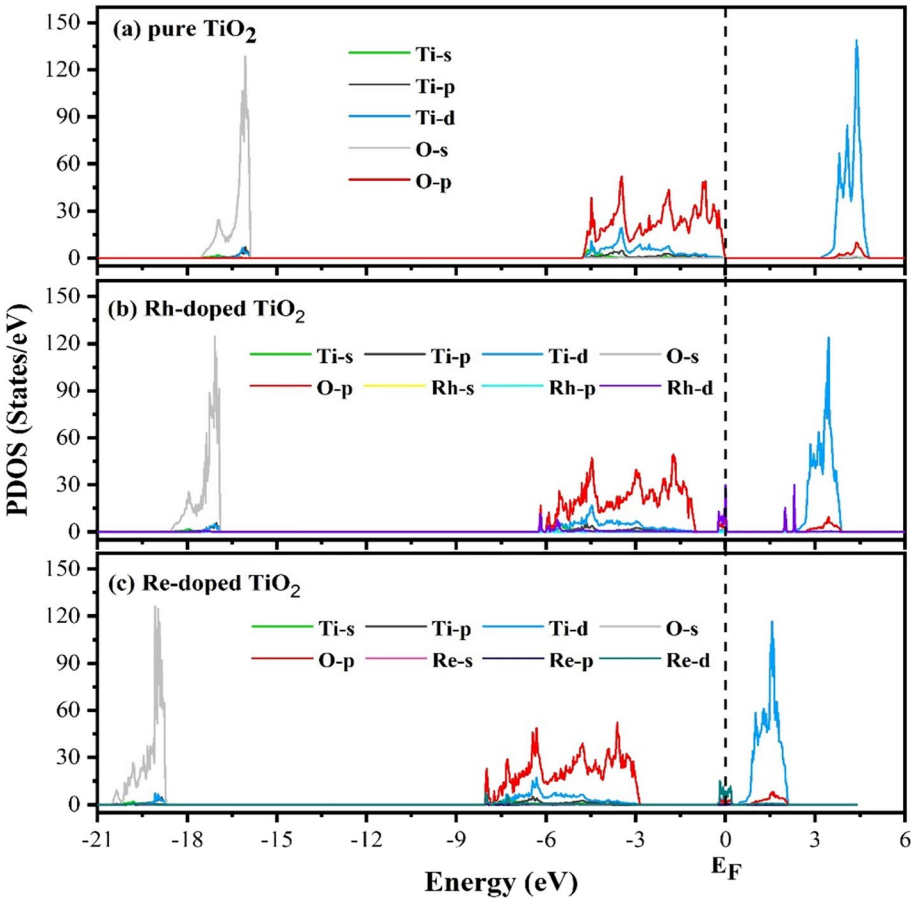

Fig. 4 PDOS of the **a** pure, **b** Rh, and **c** Re-doped TiO_2

3.2 Optical properties

Given that TiO_2 plays a vital role in optoelectronic devices, examining the impact of Rh/Re doping within the TiO_2 lattice becomes crucial. Numerous optical properties, including the refractive index, dielectric function, energy loss function, absorption coefficient, conductivity, and reflectivity, serve to clarify the complex interaction between light and matter. These properties collectively contribute to a deeper comprehension of the behavior of materials when exposed to light, thereby influencing their potential applications in optoelectronics.

The optical characteristics of a solid can be explained using its dielectric function ε, which delineates how the material reacts linearly to electromagnetic radiation. Consequently, it governs the way radiation propagates within a medium. For a static field, 'e' takes on a real value, while in the context of a dynamic field, it becomes a complex function expressed as follows: $\varepsilon(\omega) = \varepsilon_1(\omega) + i\,\varepsilon_2(\omega)$, where $\varepsilon_1(\omega)$ represents the real part and $\varepsilon_2(\omega)$ signifies the imaginary part. These functions are dependent on the frequency of the field or the energy of the photon (Biskri et al. 2016). The dielectric function, a fundamental

macroscopic property of materials, serves as a foundation for deducing various other properties. It delineates how a material reacts to an external electromagnetic (EM) field that varies with time. The reaction to an external field (or photons) across the spectrum from far-infrared to ultraviolet bands can be ascribed to various mechanisms. These encompass impurity effects, optical phonons, free carriers, excitons, and inter-band electronic transitions. The significance of each mechanism varies based on the wavelength and the specific material under consideration (Bao and Ruan 2010). The $\varepsilon_2(\omega)$ characterizes the optical absorption within the crystal. It can be computed by evaluating the momentum matrix elements between occupied and unoccupied electronic states within the first Brillouin zone (Biskri et al. 2016). Furthermore, $\varepsilon_2(\omega)$ obtained through the definition of direct transition probability, primarily describes the electron transitions from occupied states to unoccupied states. Meanwhile, the peaks in the imaginary component signify specific energy levels where electrons uptake energy, transitioning from lower (valence) to higher (conduction) energy states. This process typically involves the absorption of photons or electromagnetic radiation. (Yu et al. 2012). According to the Kramers–Kronig relationship, $\varepsilon_1(\omega)$ can be derived by integrating over a considerably wide frequency range, utilizing the differential coefficient of $\varepsilon_2(\omega)$ (Bao and Ruan 2010):

$$\varepsilon_2 = \left(\frac{C_1}{\omega^2}\right) \sum_{V.C} \int_{BZ} d^3K \frac{2}{2\pi} \left|e.M_{CV}(K)\right|^2 \delta\left[E_C(K) - E_V(K) - \hbar\omega\right]$$

$$\varepsilon_2 = 1 + C_2 \sum_{V.C} \int_{BZ} d^3K \frac{2}{2\pi} \frac{\left|e.M_{CV}(K)\right|^2}{\left[E_C(K) - E_V(K)\right]} \frac{\hbar^3}{\left[E_C(K) - E_V(K)\right]^2 - \hbar^2\omega^2}$$

Herein, C and V represent the conduction and valence bands, respectively. BZ refers to the first Brillouin zone, K is the electron wave vector, $\left|e.M_{CV}(K)\right|^2$ is the momentum transition matrix element, ω is the angular frequency, C_1 and C_2 are constants, and $E_C(K)$ and $E_V(K)$ denote the inherent energy levels of the conduction and valence bands, respectively.

To discern the impact of Rh/Re doping, it is essential to compare these optical properties between the pure TiO_2 and their doped counterparts, as portrayed in Fig. 5. This comparative analysis offers valuable insights into how the introduction of dopants influences the optical behavior of materials, paving the way for enhanced optoelectronic applications. The utilization of Maxwell's equations proves informative, allowing us to derive various optical properties directly from the complex dielectric function.

The real component of the dielectric function clarifies polarization phenomena, while the imaginary component illustrates the energy dissipation taking place within the system. Figure 5a, b illustrate the $\varepsilon_1(\omega)$ and the $\varepsilon_2(\omega)$. In low-energy regions, the real component of the dielectric function exhibits a rise alongside photon energy, culminating in its peak magnitude around the point where the energy reaches approximately ~ 4.38 eV. Beyond this particular energy threshold, the $\varepsilon_1(\omega)$ experiences a sharp decline and drops below 0 near 5.0 eV. The drop of $\varepsilon_1(\omega)$ below zero gives a negative value, which signifies a situation where the incoming photon beam loses intensity due to energy dissipation into the medium, leading to the emergence of metallic characteristics. The drop of $\varepsilon_1(\omega)$ from its maximum value can be correlated with the ascent of $\varepsilon_2(\omega)$, implying the occurrence of inter-band transitions (Ezzeldien et al. 2021).

The highest peaks in the real part occur at energy levels of 4.3 eV for pure TiO_2, 4.34 eV for Rh-doped TiO_2, and 4.4 eV for Re-doped TiO_2. These peaks signify electron transitions from the valence band's peak to the conduction band's lowest point.

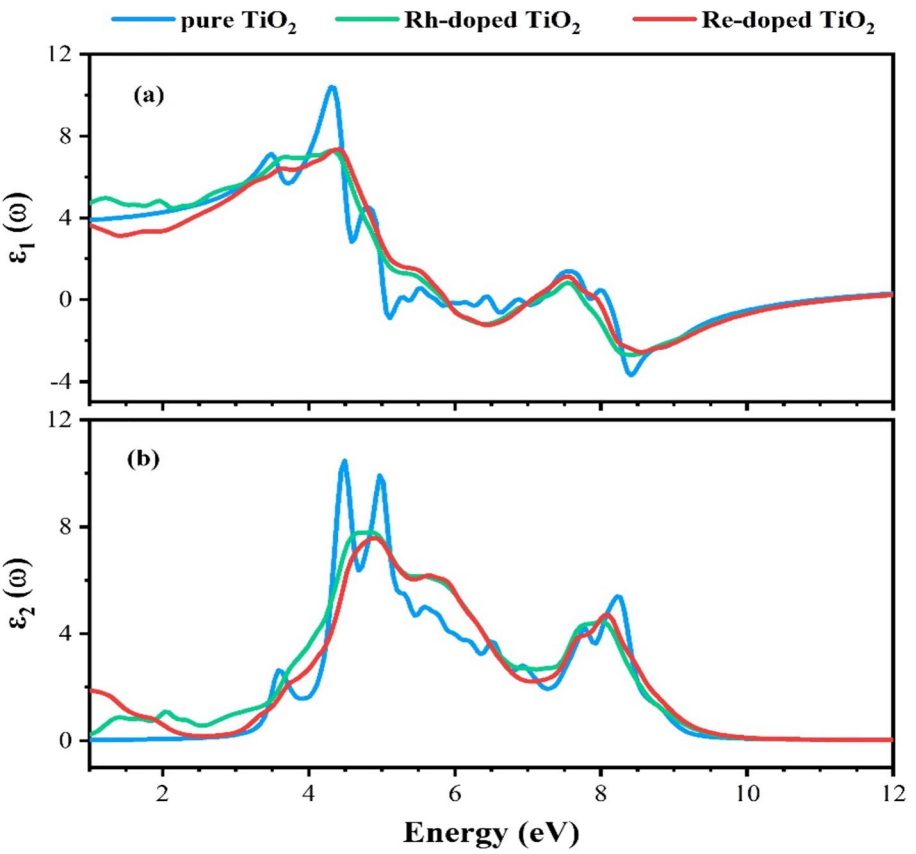

Fig. 5 **a** the ε_1 and **b** ε_2 parts of the dielectric function of the pure and Rh(Re) doped TiO_2

The redshift occurs because of a narrowing of the band gap, leading to a rise in intensity as electronic transitions increase (Rizwan et al. 2024; Ayub et al. 2024). The $\varepsilon_2(\omega)$ value is zero at 0 eV for the pure TiO_2 sample, signifying the absence of energy dissipation (absorption) within undoped TiO_2. In contrast, the doped system exhibits a positive $\varepsilon_2(\omega)$ value, indicating energy dissipation even at 0 eV. The $\varepsilon_2(\omega)$ curve highlights four prominent peaks observed at energy levels of 3.25, 4.48, 4.98, and 5.72 eV for the pure TiO_2 sample, corresponding to the absorption at these energy levels.

Based on the absorbance spectrum of pure and Rh(Re) doped TiO_2 presented in Fig. 6a, pure TiO_2 exhibits noteworthy absorption features. Notably, the absorbance profile reveals distinct absorption peaks at around 246 and 265 nm. However, two noteworthy observations are evident in the Rh(Re) doped TiO_2. Firstly, there is a noticeable shift in the absorption peaks towards lower energy levels. Secondly, the sharpness of the peaks is diminished, which could potentially be attributed to mixed transitions. These observations collectively highlight the intricate changes in the optical behavior of the material due to Rh(Re) doping, pointing towards a modification in the underlying electronic structure and interaction with light. The optical absorption peaks can be correlated with the electronic transitions between Ti-d3 and O-2p, as well as Rh-4d (Re-5d) states (Ahmed et al. 2021).

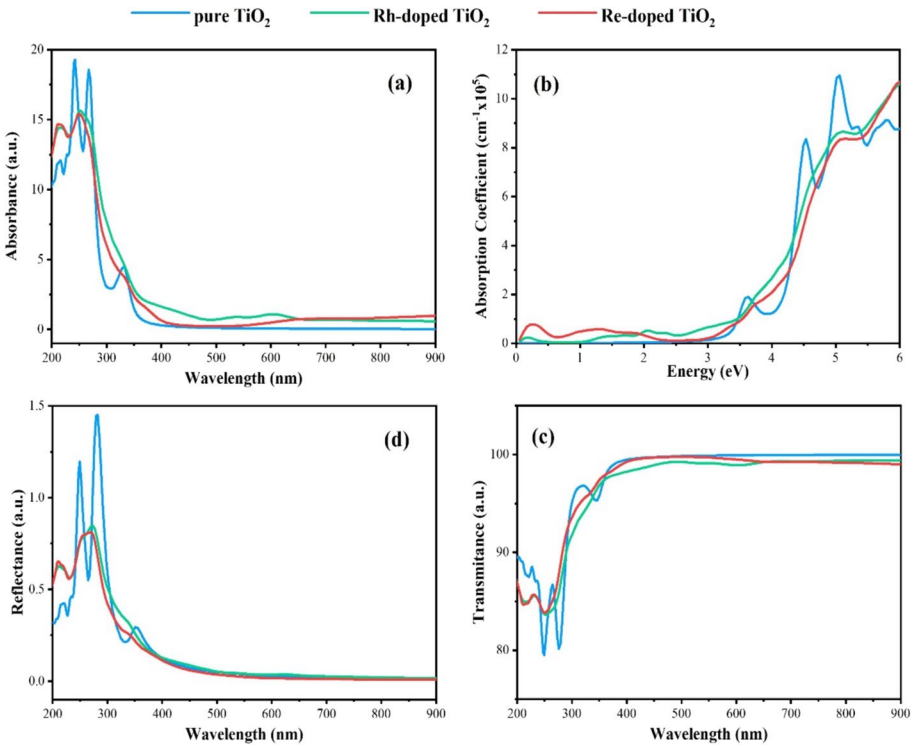

Fig. 6 **a** absorbance spectrum, **b** absorption coefficient, **c** transmittance, and **d** reflectance of the pure and Rh(Re) doped TiO_2

From the relation between the absorption coefficient and incident energy shown in Fig. 6b, it is noteworthy that the absorption edge of (Rh-Re)-doped TiO_2 shifts to lower energy compared to that of pure TiO_2. This shifting can be explained based on a considerable reduction in the energy band gap, as evidenced in Fig. 3. A noteworthy pattern emerges when comparing the transmittance and reflectance spectra of the present samples, depicted in Fig. 6c and d, respectively. The outcomes indicate that the transmittance is maximized over the whole points where the reflectance (absorbance) is minimized. This observation underscores a strong correlation between these optical properties. Furthermore, it is evident that doping significantly alters the optical absorption spectra of TiO_2.

The complex refractive index, consisting of the refractive index (n(ω)) and extinction coefficient (k(ω)), plays a crucial role in linking the electronic and optical characteristics of materials. Studying the complex refractive index gains access to a comprehensive understanding of the underlying electronic structure, allowing them to predict how a material interacts with light across a range of energies or frequencies. This insight aids in designing and optimizing materials for various applications, such as photovoltaics, optoelectronics, and sensors (Abdullah et al. 2015; Abdulwahid et al. 2016). Using the acquired $\varepsilon_1(\omega)$ and $\varepsilon_2(\omega)$, the refractive indices and extinction coefficients were computed. The subsequent relationships between the dielectric function and complex refractive index underscore the significance of the optical dielectric function in determining n and k as shown below (Rocquefelte et al. 2004):

$$n = \frac{1}{\sqrt{2}}\left[\varepsilon_1 + \sqrt{\varepsilon_1^2 + \varepsilon_2^2}\right]^{1/2}$$

$$k = \frac{1}{\sqrt{2}}\left[\sqrt{\varepsilon_1^2 + \varepsilon_2^2} - \varepsilon_1\right]^{\frac{1}{2}}$$

Figure 7a, b illustrates the spectra of n(ω) and k(ω) for the pure and Rh(Re) doped TiO_2. In both pristine and doped TiO_2 samples, the n(ω) exhibited a decline in values with longer wavelengths, whereas it displayed an ascent with shorter wavelengths. This decreasing trend can be attributed to the optical dispersion characteristics of the materials (Hussain et al. 2023). In the case of Re-doped TiO_2 and pure TiO_2, the static n values are determined to be 2.21 and 1.97, respectively. This observed increase in the static n values towards higher values upon Re-doping corroborates the shift of TiO_2's semiconducting nature towards that of a metallic material. This transformation was further substantiated by the considerable reduction in the energy band gap, as illustrated in Fig. 3b, which will support this finding.

An association exists between k(ω) and the absorption spectrum, wherein the absorption spectrum explains the absorption of energy within materials when subjected to light of specific energies. Consequently, the k(ω) value quantifies the extent of light absorption in TiO_2

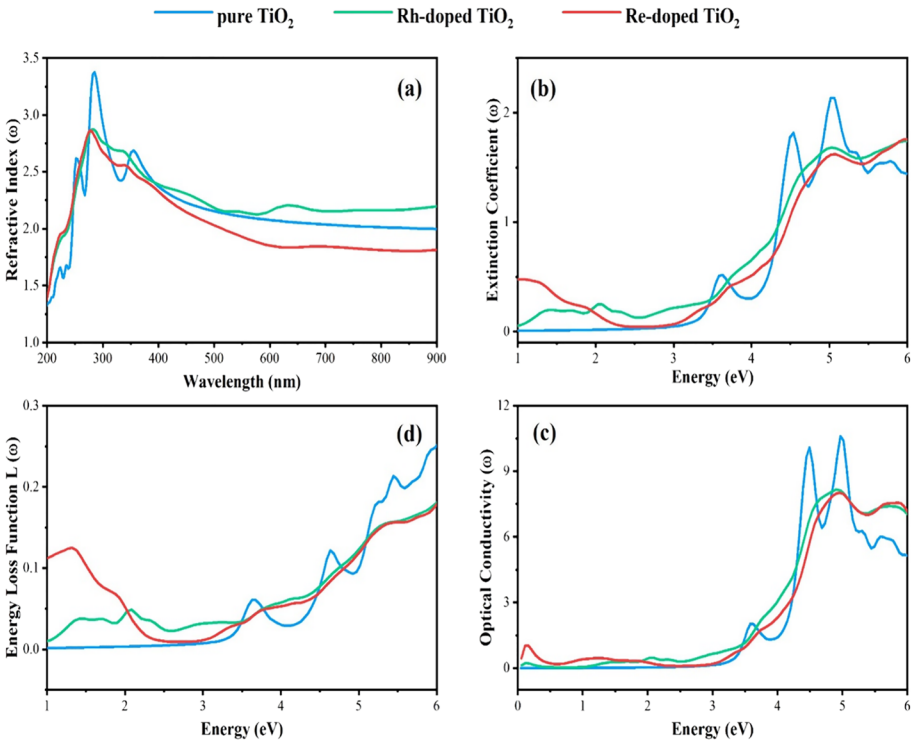

Fig. 7 **a** Refractive index, **b** extinction coefficient, **c** conductivity, and **d** energy loss function of the pure and Rh(Re) doped TiO_2

after modification by doping. A material is considered transparent when its extinction coefficient, K(ω), is zero at a specific wavelength. Conversely, when K(ω) is unity or higher, the material exhibits stronger absorption, which is a characteristic feature of metals (Fatima et al. 2023). In the case of pure TiO_2, it is evident that the k(ω) remains at zero for photon energy up to ~ 2 eV, which is related to its band gap. This absence of k(ω) results in zero absorption. This observation underscores the alignment between k(ω) and the absorption spectrum. As the value of k(ω) increases, the absorption also increases, and conversely. For instance, the k(ω) value that is closest to its highest value correlates to maximum absorption, and it subsequently falls as the material's absorption further declines. Also, it was clear that the intensity of a series of sharp peaks for pure TiO_2 sample localizing at 3.32, 4.26, and 5.04 eV was reduced significantly upon incorporating Rh and Re to the matrix, which can be attributed to the interaction between the dopants and the TiO_2 matrix, and the change in the electronic structure of composites (Li 2015).

Semiconductor optical conductivity is the state in which the conductivity process is caused by illumination. The photoconductive phenomenon is the physical process that can be exploited in optoelectronic applications of semiconductors (Yu et al. 2012; Sumanth et al. 2022). This phenomenon can be explained based on the real component of the optical conductivity (σ(ω)) shown in Fig. 7c. In the case of pure TiO_2, for instance, when the photon energy remains below 2.5 eV, the optical conductivity registers at a value of 0. As the incident photon energy reached 3 eV, a series of distinct peaks appeared, and the conductivity reached its maximum value in the vicinity of 5 eV. The intensity of σ(ω) peak decreases upon incorporating Rh(Re)-dopant to the matrix, supporting the result of $\varepsilon_2(\omega)$.

Figure 7d shows the theoretical energy loss function (L(ω)) calculated from DFT for the pure and Rh(Re) doped TiO_2. The plasma frequency (maximum value of energy loss function) for both structures (Rh-doped TiO_2 and Re-doped TiO_2) decreases. The highest of the energy loss function corresponds to an energy range where electrons, often not constrained or localized to their lattice sites, undergo plasma oscillations in response to light exposure (Cherqui et al. 2016; Aziz et al. 2017).

4 Conclusions

From the insights of this study, it has appeared that incorporating Rh-Re TMS into the TiO2 is a novel approach to alter the structural, electronic, and optical properties of the resulting TiO_2 doped matrix. These modifications have been validated through the utilization of first-principles calculations grounded in DFT. The effective manipulation of TiO_2's electronic band structure via Rh-Re doping is effectively showcased by comparing the band structures and partial density of states (PDOS) before and after doping. This comparison relies on well-established principles in the analysis of band structures. The theoretical assessment of the band gap and optical characteristics pertaining to the pure and doped samples exhibits a noteworthy concurrence with the experimental results. The emergence of Rh-Re density of states contributes to a reduction in the optical band gap after doping, from 3.20 eV for pure TiO_2 to 1.90 and 0.20 eV for Rh-doped and Re-doped TiO_2, respectively; this, in turn, results in a pronounced redshift in the absorption edge of TiO_2 upon the introduction of dopants.

Acknowledgements The authors extend their appreciation to the Ministry of Higher Education and Scientific Research, Kurdistan Regional Government, Department of Physics—College of Science—University of Sulaimani for all support and facilities provided to this work.

Author contributions TYA: Data curation, Formal analysis, Writing—review and editing. OGA: Writing—original draft, Visualization, Conceptualization, Writing—review and editing. SMM: Validation, Writing—review and editing. SBA: Conceptualization, Investigation, Formal analysis, Writing—review and editing.

Funding This research received no external funding.

Data availability statement The data will be made available by the corresponding author upon request.

Declarations

Conflict of interest The authors declare that they have no known competing financial interests or personal relationships that could have appeared to influence the work reported in this paper.

References

Abdullah, O.G., Aziz, S.B., Omer, K.M., Salih, Y.M.: Reducing the optical band gap of polyvinyl alcohol (PVA) based nanocomposite. J. Mater. Sci. Mater. Electron. **26**, 5303–5309 (2015)

Abdulwahid, R.T., Abdullah, O.G., Aziz, S.B., Hussein, S.A., Muhammad, F.F., Yahya, M.Y.: The study of structural and optical properties of PVA:PbO2 based solid polymer nanocomposites. J. Mater. Sci. Mater. Electron. **27**, 12112–12118 (2016)

Ahmed, R.M., Hasan, I.: A review on properties and applications of TiO2 and associated nanocomposite materials. Mater. Today Proc. **81**, 1073–1078 (2023)

Ahmed, F., Kanoun, M.B., Awada, C., Jonin, C., Brevet, P.F.: An experimental and theoretical study on the effect of silver nanoparticles concentration on the structural, morphological, optical, and electronic properties of TiO2 nanocrystals. Crystals **11**, 1488 (2021)

Anisimov, V.I., Zaanen, J., Andersen, O.K.: Band theory and mott insulators: Hubbard *U* instead of stoner *I*. Phys. Rev. B **44**, 943 (1991)

Armakovic, S.J., Savanovic, M.M., Armakovic, S.: Titanium dioxide as the most used photocatalyst for water purification: an overview. Catalysts **13**, 26 (2023)

Ayub, A., Ullah, H.M.N., Rizwan, M., Zafar, A.A., Usman, Z., Hira, U.: Impact of Zn alloying on structural, mechanical anisotropy, acoustic speeds, electronic, optical, and photocatalytic response of KMgF3 perovskite material. Mater. Sci. Semicon. Proc. **173**, 108049 (2024)

Aziz, S.B., Abdullah, O.G., Saber, D.R., Rasheed, M.A., Ahmed, H.M.: Investigation of metallic silver nanoparticles through UV-Vis and optical micrograph techniques. Int. J. Electrochem. Sci. **12**, 363–373 (2017)

Bao, H., Ruan, X.: Ab initio calculations of thermal radiative properties: the semiconductor GaAs. Int. J. Heat Mass Tran. **53**, 1308–1312 (2010)

Biskri, Z.E., Rached, H., Bouchear, M., Rached, D., Aida, M.S.: A comparative study of structural stability and mechanical and optical properties of fluorapatite (Ca5(PO4)3F) and lithium disilicate (Li2Si2O5) components forming dental glass–ceramics: first principles study. J. Electron. Mater. **45**, 5082–5095 (2016)

Chen, W., Yuan, P., Zhang, S., Sun, Q., Liang, E., Jia, Y.: Electronic properties of anatase TiO2 doped by lanthanides: a DFT+U study. Physica B **407**, 1038–1043 (2012)

Chen, H., Li, X., Wan, R., Kao-Walter, S., Lei, Y.: A DFT study of the electronic structures and optical properties of (Cr, C) co-doped rutile TiO2. Chem. Phys. **501**, 60–67 (2018)

Cherqui, C., Thakkar, N., Li, G., Camden, J.P., Masiello, D.J.: Characterizing localized surface plasmons using electron energy-loss spectroscopy. Annu. Rev. Phys. Chem. **67**, 331–357 (2016)

Coronado, D.R., Gattorno, G.R., Pesqueira, M.E.E., Cab, C., Coss, R.D., Oskam, G.: Phase-pure TiO2 nanoparticles: anatase, brookite and rutile. Nanotechnology **19**, 145605 (2008)

Eddy, D.R., Permana, M.D., Sakti, L.K., Sheha, G.A.N., Solihudin, S. H., Takei, T., Kumada, N., Rahayu, I.: Heterophase polymorph of TiO2 (anatase, rutile, brookite, TiO2 (B)) for efficient photocatalyst: fabrication and activity. Nanomaterials **13**, 704 (2023)

Ezzeldien, M., Al-Qaisi, S., Alrowaili, Z.A., Alzaid, M., Maskar, E., Es-Smairi, A., Vu, T.V., Rai, D.P.: Electronic and optical properties of bulk and surface of CsPbBr3 inorganic halide perovskite a first principles DFT 1/2 approach. Sci. Rep. **11**, 20622 (2021)

Farzaneh, A., Javidani, M., Esrafili, M.D., Mermer, O.: Optical and photocatalytic characteristics of Al and Cu doped TiO2: Experimental assessments and DFT calculations. J. Phys. Chem. Solids **161**, 110404 (2022)

Fatima, A., Ullah, H.M.N., Rizwan, M., Maqbool, S., Idrees, F., Usman, Z.: Theoretical description of structural, electronic, elastic, mechanical, and optical response of Ba1−xCdxTiO3 for optoelectronic applications. Mater. Today Commun. **35**, 105925 (2023)

Ghuman, K.K., Singh, C.V.: A DFT + U study of (Rh, Nb)-codoped rutile TiO2. J. Phys. Condens. Matter **25**, 085501 (2013)

Hafner, J.: Materials simulations using VASP—a quantum perspective to materials science. Comput. Phys. Commun. **177**, 6–13 (2007)

Hafner, J.: Ab-initio simulations of materials using VASP: density-functional theory and beyond. J. Comput. Chem. **29**, 2044–2078 (2008)

Hoffmann, M.R., Martin, S.T., Choi, W., Bahnemann, D.W.: Environmental applications of semiconductor photocatalysis. Chem. Rev. **95**, 69–96 (1995)

Howard, C.J., Sabine, T.M., Dickson, F.: Structural and thermal parameters for rutile and anatase. Acta Cryst. B **47**, 462–468 (1991)

Hussain, A., Rauf, A., Ahmed, E., Khan, M.S., Mian, S.A., Jang, J.: Modulating optoelectronic and elastic properties of anatase TiO2 for photoelectrochemical water splitting. Molecules **28**, 3252 (2023)

Kondamareddy, K.K., Neena, D., Lu, D., Peng, T., Lopez, M.A.M., Wang, C., Yu, Z., Cheng, N., Fu, D.J., Zhao, X.Z.: Ultra-trace (parts per million-ppm) W^{6+} dopant ions induced anatase to rutile transition (ART) of phase pure anatase TiO2 nanoparticles for highly efficient visible light-active photocatalytic degradation of organic pollutants. Appl. Surf. Sci. **456**, 676–693 (2018)

Li, W.: Influence of electronic structures of doped TiO2 on their photocatalysis. Phys. Status Solidi **9**, 10–27 (2015)

Liu, R., Zhou, X., Yang, F., Yu, Y.: Combination study of DFT calculation and experiment forphotocatalytic properties of S-doped anatase TiO2. Appl. Surf. Sci. **319**, 50–59 (2014)

Liu, X., Wang, Y., Wang, Y., Zhao, Y., Yu, J., Shan, X., Tong, Y., Lian, X., Wan, X., Wang, L., Tian, P., Kuo, H.C.: Recent advances in perovskites-based optoelectronics. Nanotechnol. Rev. **11**, 3063–3094 (2022)

Ma, D., Li, J., Liu, A., Chen, C.: Carbon gels-modified TiO2: Promising materials for photocatalysis applications. Materials **13**, 1734 (2020)

Ma, H., Sauer, J.: Computational studies of dopant effects on the photocatalytic activity of anatase TiO2. Phys. Chem. Chem. Phys. (2013)

Maeda, M., Yamada, T.: Photocatalytic activity of metal-doped titanium oxide films prepared by sol-gel process. J. Phys. Conf. Ser. **61**, 755 (2007)

Mazierski, P., Caicedo, P.N.A., Grzyb, T., Mikolajczyk, A., Roy, J.K., Wyrzykowska, E., Wei, Z., Kowalska, E., Puzyn, T., Zaleska-Medynska, A., Nadolna, J.: Experimental and computational study of Tm-doped TiO2: The effect of Li^{+} on Vis-response photocatalysis and luminescence. Appl. Catal. B Environ. **252**, 138–151 (2019)

Monkhorst, H.J., Pack, J.D.: Special points for brillouin-zone integrations. Phys. Rev. B **13**, 5188 (1976)

Muthukrishnan, S., Vidya, R., Sjastad, A.O.: Band gap engineering of anatase TiO2 by ambipolar doping: A first principles study. Mater. Chem. Phys. **299**, 127467 (2023)

Nair, R.V., Gummaluri, V.S., Matham, M.V., Vijayan, C.: A review on optical bandgap engineering in TiO2 nanostructures via doping and intrinsic vacancy modulation towards visible light applications. J. Phys. D Appl. Phys. **55**, 313003 (2022)

Niishiro, R., Konta, R., Kato, H., Chun, W.J., Asakura, K., Kudo, A.: Photocatalytic O2 evolution of rhodium and antimony-codoped rutile-type TiO2 under visible light irradiation. J. Phys. Chem. C **111**, 17420–17426 (2007)

Patil, S.B., Basavarajappa, P.S., Ganganagappa, N., Jyothi, M.S., Raghu, A.V., Reddy, K.R.: Recent advances in non-metals-doped TiO2 nanostructured photocatalysts for visible-light driven hydrogen production, CO2 reduction and air purification. Int. J. Hydrogen Energ. **44**, 13022–13039 (2019)

Perdew, J.P., Burke, K., Ernzerhof, M.: Generalized gradient approximation made simple. Phys. Rev. Lett. **77**, 3865 (1996)

Perdew, J.P., Ruzsinszky, A., Csonka, G.I., Vydrov, O.A., Scuseria, G.E., Constantin, L.A., Zhou, X., Burke, K.: Restoring the density-gradient expansion for exchange in solids and surfaces. Phys. Rev. Lett. **100**, 136406 (2008)

Raia, M.Y., Masrour, R., Hamedoun, M., Kharbach, J., Rezzouk, A., Hourmatallah, A., Benzakour, N., Bouslykhane, K.: Study of optical, magnetic, electronic, thermodynamic and mechanical properties of effect of substitution Co on Ti site on half metallicity of XA type ordering of Ti2FeGe compound. Opt. Quant. Electron. **55**, 641 (2023)

Rasul, S.M., Saber, D.R., Aziz, S.B.: Role of titanium replacement with Pd atom on band gap reduction in the anatase titanium dioxide: First-principles calculation approach. Results Phys. **38**, 105688 (2022)

Rhenium, I.L.S.: Ultra-high temperature materials I: carbon (graphene/graphite) and refractory metals, pp. 317–357 (2014)
Rizwan, M., Naeem, H., Ullah, H.M.N., Usman, Z., Amjed, N.A., Abid, M.: Fine band gap tuning via Sr incorporated PbTiO3 for optoelectronic application: a DFT study. Opt. Quant. Electron. **56**, 122 (2024)
Rocquefelte, X., Goubin, F., Koo, H.J., Whangbo, M.H., Jobic, S.: Investigation of the origin of the empirical relationship between refractive index and density on the basis of first principles calculations for the refractive indices of various TiO2 phases. Inorg. Chem. **43**, 2246–2251 (2004)
Ruiz, E.P.E., Lago, J.L., Thirumuruganandham, S.P.: Experimental studies on TiO2 NT with metal dopants through co-precipitation, sol–gel, hydrothermal scheme and corresponding computational molecular evaluations. Materials **16**, 3076 (2023)
Samsudin, E.M., Hamid, S.B.A.: Effect of band gap engineering in anionic-doped TiO2 photocatalyst. Appl. Surf. Sci. B **391**, 326–336 (2017)
Sarkar, J., Talukdar, A., Debnath, P., Chatterjee, S.: Study of bromine substitution on band gap broadening with consequent blue shift in optical properties and efficiency optimization of lead-free CsGeIXBr3−X based perovskite solar cells. J. Comput. Electron. **22**, 1075–1088 (2023)
Schwarz, W.H.E.: The full story of the electron configurations of the transition elements. J. Chem. Educ. **87**, 444–448 (2010)
Sharma, S.B., Qattan, I.A., Jaoude, M.A., Abedrabbo, S.: First-principles DFT study of structural, electronic and optical properties of Cu-doped TiO2 (112) surface for enhanced visible-light photocatalysis. Comp. Mater. Sci. **218**, 111952 (2023)
Sumanth, A., Ganapathi, K.L., Rao, M.S.R., Dixit, T.: A review on realizing the modern optoelectronic applications through persistent photoconductivity. J. Phys. D Appl. Phys. **55**, 393001 (2022)
Taylor, S.E., Bruneval, F.: Understanding and correcting the spurious interactions in charged super-cells. Phys. Rev. B **84**, 075155 (2011)
Tesch, R., Kowalski, P.M.: Hubbard *U* parameters for transition metals from first principles. Phys. Rev. B **105**, 195153 (2022)
Tian, F.H., Liu, C.B.: DFT description on electronic structure and optical absorption properties of anionic S-doped anatase TiO2. J. Phys. Chem. B **110**, 17866–17871 (2006)
Ullah, M.A., Rizwan, M., Riaz, K.N.: Innovative complex perovskites for efficient hydrogen Evolution: A DFT-Based design strategy. Mater. Sci. Eng. B **301**, 117195 (2024)
Verma, R., Gangwar, J., Srivastava, A.K.: Multiphase TiO2 nanostructures: A review of efficient synthesis, growth mechanism, probing capabilities, and applications in bio-safety and health. RSC Adv. **7**, 44199–44224 (2017)
Williamson, B.A.D., Buckeridge, J., Brown, J., Ansbro, S., Palgrave, R.G., Scanlon, D.O.: Engineering valence band dispersion for high mobility p-type semiconductors. Chem. Mater. **29**, 2402–2413 (2017)
Ye, H., Zuo, G., Cao, Y.: DFT computation of rare earth element doped TiO2 anatase: Tunable absorption spectra for water splitting application. Chem. Phys. Lett. **828**, 140720 (2023)
Yu, L., Li, D., Zhao, S., Li, G., Yang, K.: First principles study on electronic structure and optical properties of ternary GaAs: Bi alloy. Materials **5**, 2486–2497 (2012)
Yu, X., Hou, T., Li, Y., Sun, X., Lee, S.T.: Effective band gap reduction of titanium oxide semiconductors by codoping from first-principles calculations. Int. J. Quantum Chem. **113**, 2546–2553 (2013)
Yu, D., Zhou, W., Liu, Y., Zhou, B., Wu, P.: Density functional theory study of the structural, electronic and optical properties of C-doped anatase TiO2(101) surface. Phys. Lett. A **379**, 1666–1670 (2015)
Zhang, S., Wei, S., Liu, Z., Li, T., Li, C., Huang, X.L., Wang, C., Xie, Z., Al-Hartomy, O.A., Al-Ghamdi, A.A., Wageh, S., Gao, J., Tang, Y., Wang, H., Wang, Q., Zhang, H.: The rise of AI optoelectronic sensors: from nanomaterial synthesis, device design to practical application. Mater. Today Phys. **27**, 100812 (2022)
Zhu, H.X., Zhou, P.X., Li, X., Liu, J.M.: Electronic structures and optical properties of rutile TiO2 with different point defects from DFT + U calculations. Phys. Lett. A **378**, 2719–2724 (2014)

Authors and Affiliations

Taha Yasin Ahmed[1] · Omed Gh. Abdullah[2] · Soran M. Mamand[2] · Shujahadeen B. Aziz[3,4]

✉ Omed Gh. Abdullah
omed.abdullah@univsul.edu.iq

Shujahadeen B. Aziz
shujahadeenaziz@gmail.com

[1] Physics Department, College of Science, University of Sulaimani, Qlyasan Street, Sulaimani 46001, Iraq

[2] Advanced Materials Research Laboratory, Physics Department, College of Science, University of Sulaimani, Qlyasan Street, Sulaimani 46001, Iraq

[3] Research and Development Center, University of Sulaimani, Qlyasan Street, Kurdistan Regional Government, Sulaymaniyah 46001, Iraq

[4] Department of Physics, College of Science, Charmo University, 46023 Chamchamal, Sulaymaniyah, Iraq